JOURNAL OF AIRCRAFT
Vol. 30, No. 2, March–April 1993

Cruise Noise of an Advanced Propeller with Swirl Recovery Vanes

James H. Dittmar*
NASA Lewis Research Center, Cleveland, Ohio 44135
and
David G. Hall†
Sverdrup Technology, Inc., Brook Park, Ohio 44142

A model SR-7A propeller was acoustically tested with and without downstream swirl recovery vanes to determine if any extra noise was caused by the interaction of the propeller wakes and vortices with these vanes. No additional noise was observed at the cruise condition over the angular range 46–130 deg. The presence of the swirl recovery vanes unloaded the propeller and resulted in small peak noise reductions. The propeller test without vanes was also used to investigate the variation of the peak propeller noise with helical tip Mach number. As observed before on other propellers, the peak noise initially increased with helical tip Mach number and remained constant or decreased at higher helical tip Mach numbers. Detailed pressure-time histories indicate that a portion of the primary pressure pulse is progressively cancelled by a secondary pulse as the helical tip Mach number is increased.

Introduction

ADVANCED turboprop-powered aircraft have the potential for significant fuel savings over equivalent core technology turbofan-powered aircraft. To investigate this potential, NASA has an ongoing advanced turboprop program. A description of this program and a bibliography of papers resulting from this program is found in Ref. 1. Both single and counter-rotation propellers have been investigated by NASA. Counter-rotation propellers have a theoretically higher efficiency than single rotation propellers because the second row of blades is able to recover some of the residual swirl left from the forward set of blades. In this investigation, a single rotation model propeller was tested with and without a fixed set of swirl recovery vanes behind the propeller. The intent of these vanes is to recover some of the residual swirl from the propeller without the added complication of a second set of rotating blades as exists in the counter-rotation propeller.

The noise generated by advanced propellers is of concern as a cabin environment problem for the airplane at cruise. Cruise noise measurements of single rotation propeller models[2–5] and counter-rotation propeller models[6–8] have been made previously in the NASA Lewis Research Center 8 × 6-ft wind tunnel. Counter-rotation propellers show an additional cruise noise component over single rotation propellers caused by the interaction of the upstream blade wakes and vortices with the downstream blades. The interaction noise can be separated from the propeller-alone tones for a counter-rotation propeller because the interaction tone occurs at a different frequency. Since the swirl recovery vanes also intercept the propeller wakes and vortices, interaction noise can be generated here also. Here, since the vanes do not rotate, the interaction noise is radiated at the propeller blade passing tone and its harmonics. As a result, this interaction noise is not separable as for the counter-rotation case and would only be seen as an increase in the total noise at each harmonic. Noise measurements were made for a single rotation propeller with and without these swirl recovery vanes to assess the amount of interaction noise that might be generated. This article presents the results of acoustic measurements taken in the NASA 8 × 6-ft wind tunnel at cruise conditions for the SR-7A propeller with and without swirl recovery vanes.

Presented as Paper 90-3932 at the AIAA 13th Aeroacoustics Conference, Tallahassee, FL, Oct. 22–24, 1990; received Jan. 16, 1991; revision received March 3, 1992; accepted for publication March 6, 1992.

*Senior Research Engineer. Member AIAA.
†Research Engineer. Member AIAA.

Apparatus and Procedure

Swirl Recovery Vanes

An eight-bladed single rotation propeller, designated SR-7A, was tested with and without swirl recovery vanes. Figure 1a is a photograph of these vanes behind the SR-7A propeller model. An individual propeller blade is shown in Fig. 1b and a swirl recovery vane is shown in Fig. 1c. This model had eight recovery vanes with a leading-edge hub-to-tip sweep of approximately 45 deg. The swirl recovery vanes were tested in two axial positions as illustrated in Fig. 2. The propeller was tested at three blade setting angles, 63.3, 60.2, and 57.7 deg, with the swirl recovery vane setting angle set at 86.1 deg. This was done at both close and far vane spacings for tunnel Mach numbers varying from 0.6 to 0.8. At the close vane spacing the propeller was also tested at the 63.3-deg blade setting angle with the vanes set at 87.5 and 84.7 deg. The propeller was also tested by itself without the swirl recovery vanes at the nominal blade setting angles of 63.3, 60.2, and 57.7 deg. In addition, the propeller was tested alone at the 60.2-deg blade setting angle at an advance ratio of 3.06 for tunnel Mach numbers of 0.6–0.86 to obtain propeller pressure-time histories.

Acoustic Measurements

A plate was mounted from the tunnel ceiling, 0.3 propeller diameters from the tip, and 0–1.03 × 10^5 N/m^2(0–15 psia) pressure transducers were installed flush with the plate surface to measure the noise. A sketch of the installed plate is shown in Fig. 3. Twelve transducers were installed on the plate centerline which was directly above the propeller centerline. The transducer locations are shown in Fig. 3. The transducers had a linear response to pressure fluctuations from 0 to 10,000 Hz and were calibrated with a standard piston phone noise source. The signals from the pressure transducers were recorded on

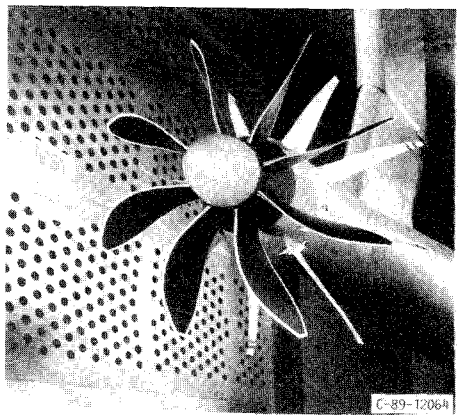

a) Propeller with swirl recovery vanes

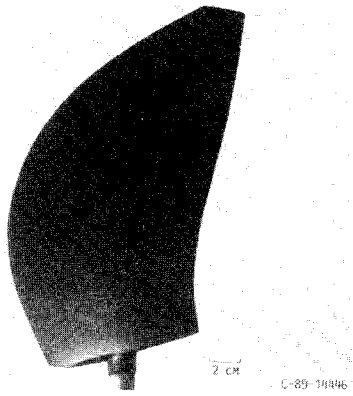

b) SR-7A propeller blade

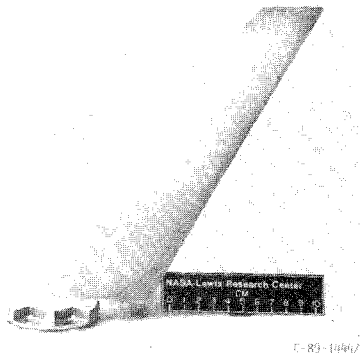

c) Swirl recovery vane

Fig. 1 Swirl recovery vane apparatus.

magnetic tape and narrow-band spectra were obtained for each of the test points. Typically the narrow-band range was 0–10,000 Hz with a bandwidth of 32 Hz. However, because the propeller blade passing frequency was so close to the wind-tunnel compressor tone at some of the test conditions, some higher resolution narrow-bands (0–2500 Hz with an 8-Hz bandwidth) were performed to isolate the propeller tone. Noise data were taken for the experimental test conditions listed in Tables 1 and 2.

The data taken at varying tunnel Mach numbers with the propeller operated at an advance ratio of 3.06 were reduced to pressure-time histories using signal enhancement with a once-per-revolution signal as the trigger. This enhancement was necessary to obtain accurate time histories because of the high level of the tunnel background noise.

Results and Discussion

Noise Variation with Swirl Recovery Vanes

The addition of the swirl recovery vanes did not show any additional interaction noise within the angular range of trans-

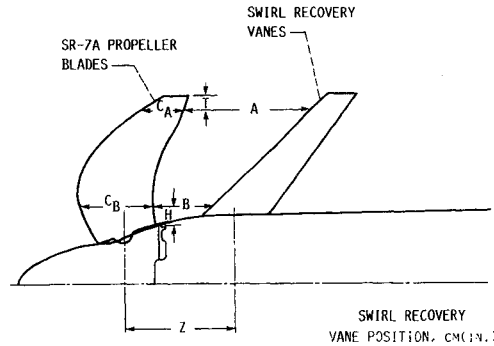

	SWIRL RECOVERY VANE POSITION, CM(IN.) CLOSE	FAR
A - DISTANCE FROM PROPELLER TRAILING EDGE TO VANE LEADING EDGE AT "T"	30.80(12 1/8)	47.00(18 1/2)
B - DISTANCE FROM PROPELLER TRAILING EDGE TO VANE LEADING EDGE AT "H"	15.24(6)	31.44(12 3/8)
C_A - PROJECTED CHORD OF PROPELLER BLADE AT "T"	3.65(1 7/16)	3.65(1 7/16)
C_B - PROJECTED CHORD OF PROPELLER BLADE AT "H"	12.07(4 3/4)	12.07 (4 3/4)
H - DISTANCE OUT FROM HUB	4.45(1 3/4)	4.45 (1 3/4)
T - DISTANCE IN FROM TIP	.95(3/8)	.95 (3/8)
Z - DISTANCE FROM PROPELLER STACKING LINE TO VANE STACKING LINE	23.80(9.38)	40.00(15 3/4)

Fig. 2 Swirl recovery vane positions.

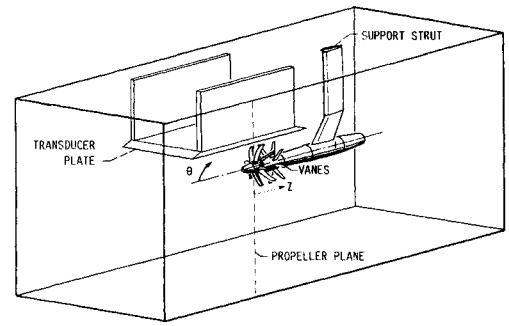

POSITION	TRANSDUCER (PLATE 0.3 DIAMETER FROM TIP)											
	1	2	3	4	5	6	7	8	9	10	11	12
	TRANSDUCER POSITION, CM (IN.)											
Z	-46.7 (-18.4)	-41.7 (-16.4)	-30.5 (-12.0)	-16.0 (-6.3)	-8.9 (-3.5)	0.8 (0.3)	8.9 (3.5)	12.4 (4.9)	18.0 (7.1)	25.0 (9.9)	28.7 (11.3)	42.4 (16.7)
	ANGLE FROM UPSTREAM, DEG											
θ	46.8	50.0	58.5	72.2	80	90.9	100	104	110	116.8	120	130.4

Fig. 3 Acoustic measurement setup.

ducer positions (46–130 deg) for any of the conditions tested. The interaction noise should theoretically peak at the far forward and far aft locations, particularly for this eight blade by eight vane configuration, and there may be some additional noise at these locations but none was observed for the existing range of transducer positions. Since the existing range of transducer positions covers the area of peak noise on the fuselage, any additional noise forward or aft of these locations is expected to have little impact on the cabin noise. Figure 4 shows the blade passing tone noise for the design condition, axial Mach number $M = 0.8$, advance ratio $J = 3.25$, blade angle = 63.3 deg, vane angle = 86.1 deg. These values were obtained from ordinary frequency domain spectra and the tone levels plotted were at least 6 dB above the broadband noise level. As can be observed, no additional noise appears to occur with the swirl recovery vanes at either the close or far positions.

The noise around the peak noise location, near the propeller plane at 90–110 deg, is even slightly diminished with the addition of the swirl recovery vanes. The differences shown here are more than the typical data scatter. These trends can be seen even more clearly at some of the off-design conditions. For example, Fig. 5 shows the data at $M = 0.75$, $J = 3.06$

Table 1 Swirl recovery vanes at 86.1 deg angle with vanes off, vanes close, and vanes far

Axial Mach number	Advanced ratio at propeller blade angle, deg		
	57.7	60.2	63.3
0.8	—	—	4.0
	—	3.75	3.75
	3.5	3.5	3.5
	3.25	3.25	3.25
	3.06	3.06	—
	2.9	—	—
0.75	—	—	4.0
	—	3.75	3.75
	3.5	3.5	3.5
	3.25	3.25	3.25
	3.06	3.06	3.06
	2.75	—	—
0.7	—	—	4.0
	3.75	3.75	3.75
	3.5	3.5	3.5
	3.25	3.25	3.25
	3.06	3.06	3.06
	—	—	—
0.65	—	—	4.0
	—	3.75	3.75
	3.5	3.5	3.5
	3.25	3.25	—
	3.06	3.06	3.06
	2.75	—	—
0.6	—	—	4.0
	—	3.75	3.75
	3.5	3.5	3.5
	3.25	3.25	3.25
	3.06	3.06	3.06
	2.75	—	—

Table 2 Propeller at 63.3-deg blade setting angle, vanes in close position

Axial Mach number	Advance ratio at vane setting angles of 84.7, 86.1, and 87.5 deg
0.8	4.0
	3.75
	3.5
	3.25
0.75	4.0
	3.75
	3.5
	3.25
	3.06
0.7	4.0
	3.75
	3.5
	3.25
	3.06
0.65	4.0
	3.75
	3.5
	3.06
0.6	4.0
	3.75
	3.5
	3.25
	3.06

for the propeller blade setting angle of 60.2 deg. Here, the noise without the vanes has the highest peak level. When the vanes are added at the far position the noise is decreased, and when the vanes are moved to the close position the noise is decreased even further.

These noise reductions appear to be reductions in the propeller loading noise as a result of the vane unloading the propeller. Figure 6 illustrates this unloading and is a plot of the propeller power coefficient C_p vs advance ratio for the noise conditions of Fig. 5. As can be seen, the addition of the vanes lowers the power coefficient. The propeller alone has the highest C_p while the propeller with the vanes in the close position has the lowest C_p. The highest C_p here in Fig. 6 corresponds to the most noise in Fig. 5, whereas, the lowest C_p corresponds to the least noise. The noise variation also followed the trend of the loading variation for the 57.7- and 63.3-deg blade setting angles.

The data shown here indicate that the swirl recovery vanes unloaded the propeller and this resulted in lower propeller noise. Increases in interaction noise from the propeller wakes and vortices impacting the swirl recovery vanes were not observed for the range of transducer positions tested. The net result of this testing is that the addition of the swirl recovery vanes can provide a small peak noise reduction for the fuselage of an airplane at cruise conditions.

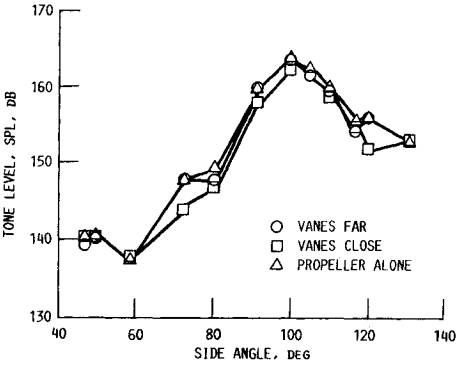

Fig. 4 Swirl recovery vane blade passing tone directivity at M = 0.8, J = 3.25, vane setting angle = 86.1 deg.

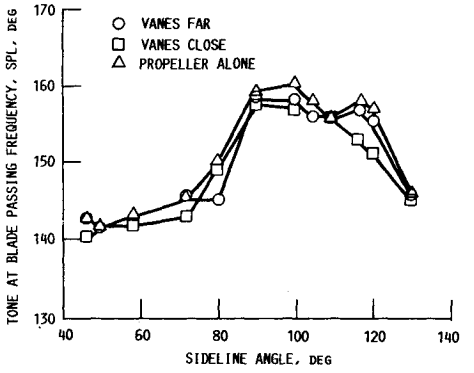

Fig. 5 Swirl recovery vane cruise noise directivity at M = 0.75, J = 3.06, blade setting angle = 60.2 deg, vane setting angle = 86.1 deg.

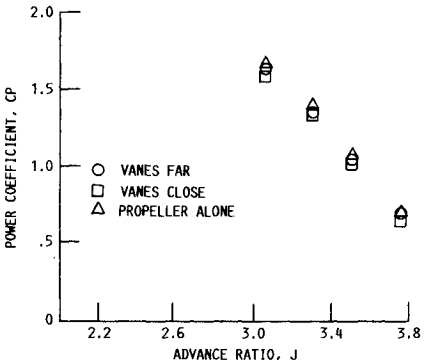

Fig. 6 Power coefficient variation with and without swirl recovery vanes, M = 0.75, SR-7A blade setting angle = 60.2 deg.

Noise Variation with Swirl Recovery Vane Blade Setting Angle

Some small peak noise variation was also observed with different swirl recovery vane blade setting angles. The experiments were performed with the vanes in the close position and the propeller blade angle set at 63.3 deg. Three vane angles were tested: 1) 84.7, 2) 86.1, and 3) 87.5 deg. Figure 7 shows the noise directivity at the design conditions of M = 0.8 and J = 3.25. The 86.1-deg blade setting angle showed the most recovered thrust of the three blade angles and the 84.7-deg angle showed the least recovered thrust. As can be seen in Fig. 7, the 86.1-deg vane angle showed the least noise, whereas, the 84.7-deg angle showed the most noise. This indicates that the better the vane performance the larger the peak noise reduction that might be achieved on the fuselage at cruise.

Propeller-Alone Pressure-Time Histories

As observed before[2] the peak propeller blade passing tone first rises with increasing helical tip Mach number and then levels off or decreases at higher helical tip Mach numbers. This can be seen in Fig. 8 for the data taken in this experiment on the SR-7A propeller model. This propeller was operated at a constant advance ratio of 3.06 so each of the helical tip Mach number points was obtained at a different tunnel axial Mach number as indicated on Fig. 8. As can be observed, the data points were taken in steps of 0.02 axial Mach number from 0.7 to 0.86 to obtain a finer variation in helical tip Mach number than was obtained in the previous experiments.

In an attempt to understand what is happening at the higher helical tip Mach numbers, pressure-time histories were obtained for the transducer signals. These were obtained by signal enhancement using a once-per-revolution signal from the propeller (synchronous time averaging). A typical pressure-time history is shown in Fig. 9. This was taken at the peak noise location at the M = 0.72, M_{ht} = 1.03 condition and represents an average of approximately 40 revolutions. The figure shows one pulse from each of the eight blades. The pulses consist of a broad positive portion and a sharp negative portion. This negative portion is larger than the positive portion and is a major contributor to the blade passing tone and its harmonics.

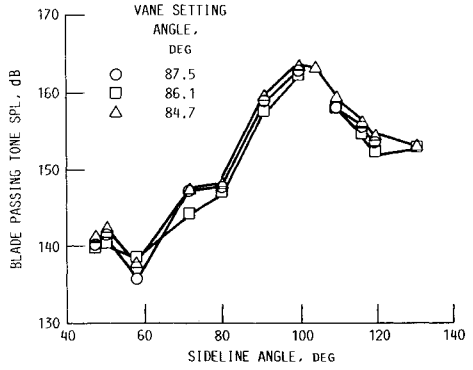

Fig. 7 Cruise noise variation with vane setting angle, M = 0.8, J = 3.25, blade setting angle = 63.3 deg.

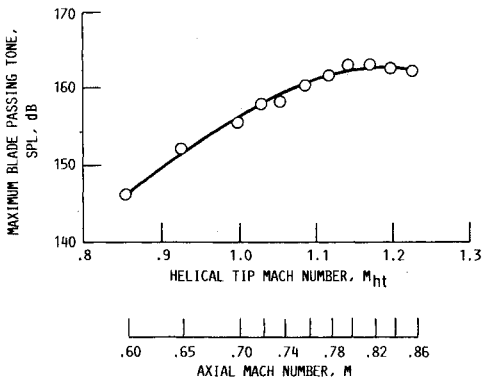

Fig. 8 Maximum blade passing tone vs helical tip Mach number at constant advance ratio of 3.06.

As the helical tip Mach number was increased to the peak noise value (Fig. 8, M = 0.8, M_{ht} = 1.15), the pressure-time history of Fig. 10 was observed. This pressure-time trace is very similar in shape to the one at M = 0.72, M_{ht} = 1.03 with a broad and slightly larger positive portion and a sharp negative portion. However, the negative portion of the pulse is showing the presence of a second positive pulse which is starting to fill in the negative portion. This is highlighted by the arrows in Fig. 10. The filling in of the negative portion of the pulse is starting to limit the growth of the blade passing tone with increasing helical tip Mach number.

As the helical tip Mach number was increased further, the second pulse became larger in strength and filled the negative pulse more completely. This can be seen in Fig. 11 which shows the pressure-time history at M = 0.86, M_{ht} = 1.23. Here the second pulse has partly filled the trough and is showing up as a second spike on the positive portion. It appears that this second pulse, with its cancelling interference on the first pulse, is the reason the peak noise does not continue to increase with helical tip Mach number. An understanding of the source of the second pulse is desirable.

During the propeller-alone testing to obtain pressure-time waveforms, one of the eight propeller blades had a shortened chord at the tip. This was a result of some previous damage to the blade. Figure 12a shows a normal blade and Fig. 12b

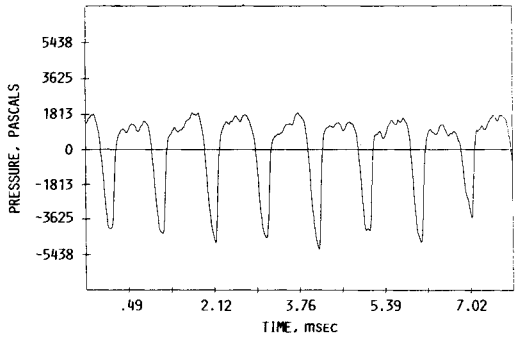

Fig. 9 Pressure-time history at M = 0.72, M_{ht} = 1.03.

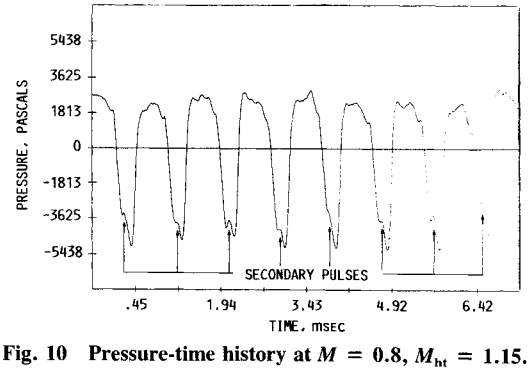

Fig. 10 Pressure-time history at M = 0.8, M_{ht} = 1.15.

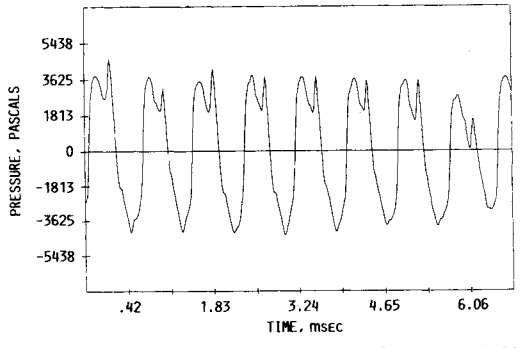

Fig. 11 Pressure-time history at M = 0.86, M_{ht} = 1.23.

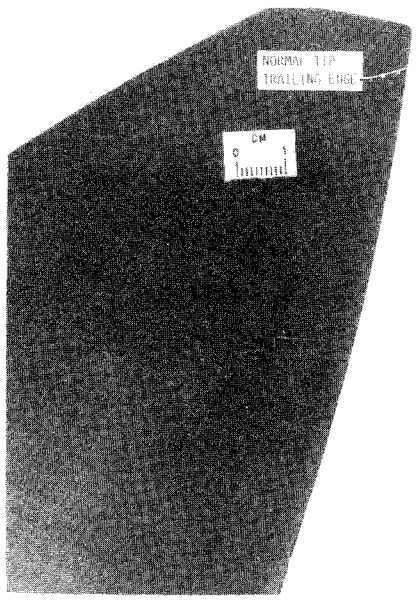

a) Normal blade tip

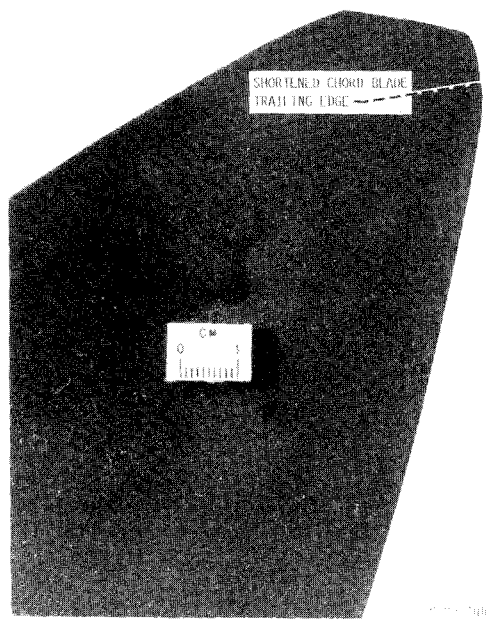

b) Blade with shortened tip chord

Fig. 12 Blade tip shape.

shows the trailing edge region of the shortened chord blade. The result of this shortened chord blade tip can be seen in the pressure-time history of Fig. 11. The last pulse on these traces is believed to be from the blade with the shortened tip chord. As can be seen from Fig. 11, the blade with the shortened tip chord has a smaller primary pressure-time signature than the other blades. This indicates that at these conditions the blade tip region is the controlling noise producing region of the blade. It can also be observed that the strength of the secondary pulse is reduced even more than the initial pulse, indicating that the secondary pulse is from the same blade as the initial pulse.

One of the possible sources considered for the secondary pulse was a reflection of an initial blade pulse from some other surface, such as the tunnel walls, the propeller hub, or another propeller blade. An examination of the trace in Fig. 11 shows that the second pulse from the shortened blade is arriving behind the initial pulse by about one-fourth of the spacing between two blades. This one-fourth blade spacing distance would then have to be the difference in distance between the direct and reflected path lengths. In viewing the

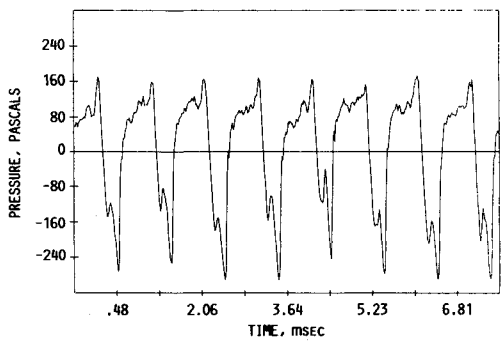

Fig. 13 Pressure-time history from SR-3 propeller on jetstar airplane at $M = 0.805$, $M_{ht} = 1.14$.

geometry, the noise path lengths to any of the possible reflecting surfaces are much larger than the distance between the primary and secondary pulses. The possibility of a direct reflection during the same revolution of the propeller is then eliminated. For the secondary pulse to be a reflection of the shortened blade's primary pulse, the reflection would then have to be arriving some whole number of revolutions of the propeller later than the initial pulse and falling back onto the same initial blade pressure pulse. Although this scenario is theoretically possible for some specific propeller speed and transducer location, the timing of the reflected pulse would vary with a change in propeller speed of transducer position and the reflected pulse would fall someplace else in the pressure-time trace. The data at other propeller speeds and other transducer locations shows the same relative timing of the initial and secondary pulses. This then eliminates the possibility that the secondary pulse is a reflection of the initial pulse from the shortened blade.

Data from other sources also show the presence of this secondary pulse in the pressure-time history. Figure 13 is the pressure-time history of the SR-3 propeller model at the peak noise location 107 deg, measured on the fuselage of the Jetstar airplane. These experiments are described in Ref. 9. The propeller was operating at an axial Mach number of 0.805 and a helical tip Mach number of 1.14. These conditions were the highest reached during the airplane test and correspond roughly to the SR-7A conditions of Fig. 10. The pressure levels are lower here than for the SR-7A traces because the microphones are farther away and the airplane is at altitude with lower air density. As can be seen on Fig. 13, the secondary pulse is beginning to fill in the initial pulse just as it did for the SR-7A trace. The presence of this interfering pulse on a different propeller in a different type of test facility shows that this phenomena is not unique to the 8 × 6 wind tunnel or to the SR-7A propeller model.

The secondary pulse is then indicated as originating on the same propeller blade as the initial pulse. The spike type nature of the secondary pulse shape is similar to that for a shock wave and may be from a trailing edge shock on the blade. The secondary pulse could also be the result of the blade spanwise loading or thickness distribution. In any case, the secondary pulse is related directly to the blade and it may be possible to improve on this cancellation or shift it to another Mach number range if desired. To do this, however, will require a deeper understanding of the secondary pulse source.

Concluding Remarks

The SR-7A model propeller was acoustically tested with and without downstream swirl recovery vanes. The swirl recovery vanes were installed in two axial positions. The propeller wakes and vortices strike the downstream vanes and create an interaction noise source which is in addition to the propeller-alone noise sources. The purpose of these experiments was to determine if this interaction noise had an effect on the total noise impacting the airplane fuselage at cruise.

The experiments showed no increase in noise at any measurement location due to the installation of the swirl recovery vanes. It is possible that the swirl recovery vane interaction noise contributes to the total noise at farther forward or father aft measurement positions but this should not significantly affect the cabin noise.

The presence of the swirl recovery vanes appears to unload the propeller. This lowers the loading noise generated by the propeller itself and results in small noise reductions. The reductions were observed near the propeller plane and corresponded to small reductions in the peak blade passing tone levels.

The swirl recovery vanes were also tested at different blade setting angles while located in the close position. Here the vane setting angle which had the best performance in recovering the propeller swirl (most thrust addition) resulted in the least noise.

The propeller-alone noise variation with helical tip Mach number was also investigated during this experiment. The propeller noise was observed to initially increase with helical tip Mach number and then level off or decrease at higher helical tip Mach numbers. In this experiment detailed pressure-time histories were measured at several closely spaced helical tip Mach numbers. At the lower helical tip Mach numbers the primary pressure pulse from a blade had a broad positive portion and a sharp negative portion. In the region where the noise vs helical tip Mach number curve starts to level off, a second pulse is observed. This second pulse starts to cancel the negative portion of the primary pulse and causes the noise to level off. This second positive pulse appears to originate on the same blade as the primary pulse and is in some way connected to the blade itself. This suggests the possibility of redesigning the blade to improve this cancellation.

References

[1]Hager, R. D., and Vrabel, D., "Advanced Turboprop Project," NASA SP-495, 1988.

[2]Dittmar, J. H., and Stang, D. B., "Cruise Noise of the 2/9th Scale Model of the Large-Scale Advanced Propfan (LAP) Propeller, SR-7A," NASA TM-100175, Sept. 1987.

[3]Dittmar, J. H., "Preliminary Measurement of the Noise from the 2/9 Scale Model of the Large-Scale Advance Propfan (LAP) Propeller, SR-7A," NASA TM-87116, Dec. 1985.

[4]Dittmar, J. H., Jeracki, R. J., and Blaha, B. J., "Tone Noise of Three Supersonic Helical Tip Speed Propellers in a Wind Tunnel," NASA TM-79167, June 1979.

[5]Dittmar, J. H., and Jeracki, R. J., "Additional Noise Data on the SR-3 Propeller," NASA TM-81736, May 1981.

[6]Dittmar, J. H., and Stang, D. B., "Noise Reduction for Model Counterrotation Propeller at Cruise by Reducing Aft-Propeller Diameter," NASA TM-88936, May 1987.

[7]Dittmar, J. H., "The Effect of Front-to-Rear Propeller Spacing on the Interaction Noise of a Model Counterrotation Propeller at Cruise Conditions," NASA TM-100121, Aug. 1987.

[8]Dittmar, J. H., Gordon, E. B., and Jeracki, R. J., "The Effect of Front-to-Rear Propeller Spacing on the Interaction Noise at Cruise Conditions of a Model Counterrotation Propeller Having a Reduced Diameter Aft Propeller," NASA TM-101329, Oct. 1988.

[9]Dittmar, J. H., "Further Comparison of Wind Tunnel and Airplane Acoustic Data for Advanced Design High Speed Propeller Models," NASA TM-86935, April 1985.